Fermi National Accelerator Laboratory

FERMILAB-Conf-98/105

Detector-Accelerator Interface Studies at the Tevatron

A.I. Drozhdin and N.V. Mokhov

Fermi National Accelerator Laboratory
P.O. Box 500, Batavia, Illinois 60510

April 1998

Published Proceedings of the *LAFEX International School on High Energy Physics Lishep98, Workshop on Diffractive Physics*, Rio de Janeiro, Brazil, February 16-20, 1998

Operated by Universities Research Association Inc. under Contract No. DE-AC02-76CH03000 with the United States Department of Energy

Disclaimer

Distribution

Detector-Accelerator Interface Studies at the Tevatron*

A. I. Drozhdin and N. V. Mokhov

Fermi National Accelerator Laboratory, P.O. Box 500, Batavia, Illinois 60510

April 10, 1998

Abstract

A summary of studies is presented towards minimization of beam loss in the critical locations at the Fermilab Tevatron to reduce background rates in the collider detectors and to protect machine components. Based on detailed Monte-Carlo simulations, measures have been proposed and incorporated in the machine to reduce accelerator-related instantaneous and residual background levels in the DØ and CDF detectors. Measurements performed are in good agreement with the predictions. Most recent results on acceptance and background rates in the DØ and CDF forward detectors are presented and discussed in detail.

1 Introduction

In Run I the Tevatron reliably provided 900×900 GeV $p\overline{p}$ collisions with a peak luminosity up to $2.5 \times 10^{31}\,\mathrm{cm}^{-2}\,\mathrm{s}^{-1}$. Work is progressing to upgrade the accelerator and detectors into even more powerful research tools in Run II [1]. The high performance of the Tevatron both in the fixed target and collider modes is achievable only with a dedicated beam cleaning system embedded in the lattice. Recent proposals to add new Forward Proton Detectors (FPD) to both DØ and CDF, which are strongly coupled with the accelerator lattice, make the detector-machine interface issues of primary concern. Only sophisticated simulations of beam loss in the interaction regions (IR) and showers induced in accelerator and detector components (resulting in increased backgrounds), along with coherent studies of detector acceptance, give a clue on the feasibility of these new detectors. The most recent results on a beam collimation system and acceptance and background rates in the DØ and CDF detectors for Run II are presented and discussed in this paper.

*Published Proceedings of the *LAFEX International School on High Energy Physics LISHEP98, Workshop on Diffractive Physics*, Rio de Janeiro, Brazil, February 16-20, 1998

2 Beam Collimation System

2.1 Scraping Beam Halo

In the Tevatron, as in any other accelerator, the creation of beam halo is unavoidable. Proton (antiproton) scattering in the interaction points (IPs), in beam-gas interactions and on the limiting apertures, the diffusion of particles due to various nonlinear phenomena out of the beam-core, as well as various hardware and software errors, all result in emittance growth and eventually in beam loss in the lattice [2, 3, 4]. This causes irradiation of conventional and superconducting (SC) components of the machine, an increase of background rates in the detectors, possible radiation damage, quench, overheating of equipment and even a total destruction of some units. A very reliable multi-component beam collimation system is the main way to control beam loss and is mandatory at any SC accelerator, providing [3, 4]:

- reduction of beam loss in the vicinity of IPs to sustain favorable experimental conditions;
- minimization of radiation impact on personnel and environment by localizing beam loss in the predetermined regions and using appropriate shielding in these regions;
- protection of accelerator components against irradiation caused by operational beam loss and enhancement of reliability of the machine;
- prevention of quenching of SC magnets and protection of other machine components from unpredictable abort and injection kicker prefires/misfires and unsynchronized abort.

In the early Tevatron days the first collimation system was designed [2] on the basis of the MARS-STRUCT [5, 6] full-scale simulations of beam loss formation in the machine. The optimized system, consisted of a set of collimators about 1 m long each, was installed in the Tevatron which immediately made it possible to raise by a factor of 5 the efficiency of the fast resonant extraction system and intensity of the extracted 800 GeV proton beam. The data on beam loss rates and on their dependence on the collimator jaw positions were in excellent agreement with the calculational predictions.

We have since refined the idea of a primary-secondary collimator set and shown that this is the only way to use such a system in the TeV region with a length of a primary collimator going down to a fraction of a radiation length. The whole system should consist then of a primary *thin scattering target*, followed immediately by *a scraper* with a few *secondary collimators* at the appropriate locations in the lattice [3, 4, 7]. The purpose of a thin target is to increase amplitude of the betatron oscillations of the halo particles and thus to increase their impact parameter on the scraper

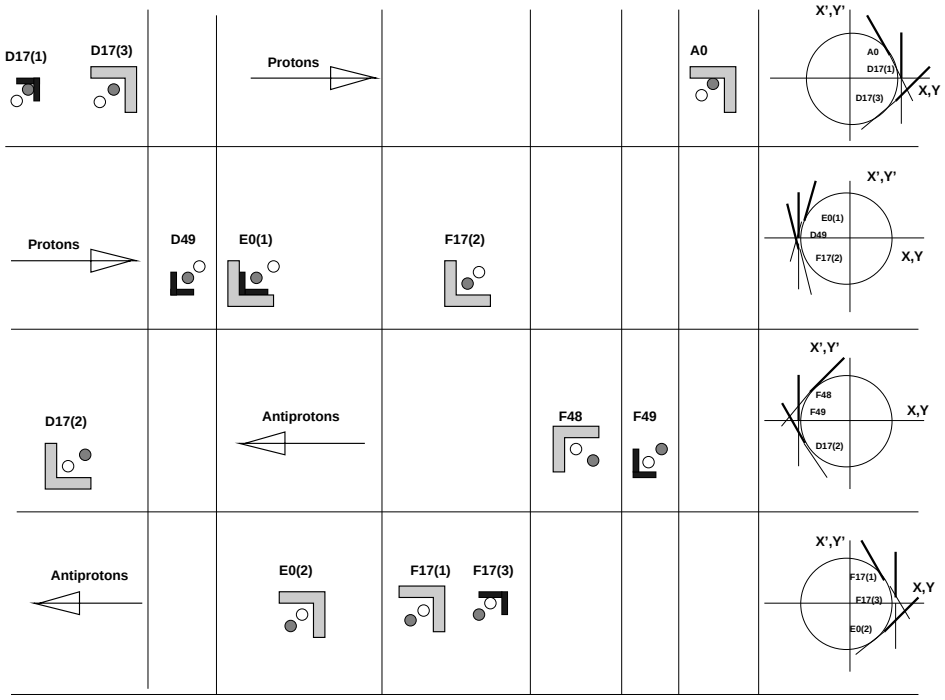

Figure 1: Tevatron Run II collimators.

face on the next turns. This results in a significant decrease of the outscattered proton yield and total beam loss in the accelerator, scraper jaws overheating and mitigating requirements to scraper alignment. Besides that, the scraper efficiency becomes almost independent of accelerator tuning, there is only one significant but totally controllable restriction of accelerator aperture and only the scraper region needs heavy shielding and probably a dogleg structure. The method would give an order of magnitude in beam loss reduction at multi-TeV machines, but even at the Tevatron we have got a noticeable effect. Recently the existing scraper at AØ was replaced with a new one with two 2.5 mm thick L-shaped tungsten targets with 0.3 mm offset relative to the beam surface on the either end of the scraper (to eliminate the misalignment problem), resulting in reduction of beam loss rate upstream of both collider detectors [8].

2.2 Beam Collimation for Tevatron Run II

A new sophisticated beam collimation system has been designed for the Tevatron Run II (Fig. 1). It consists of a set of the primary and secondary collimators both for nominal momentum and off-momentum halo interception. L-shaped primary collimators shave the proton and antiproton beams as shown in Fig. 2. Proton halo phase space at the corresponding secondary collimator is shown there also. Ellipses represent a 6σ beam envelope. A vertical line shows the location of the collimator jaw.

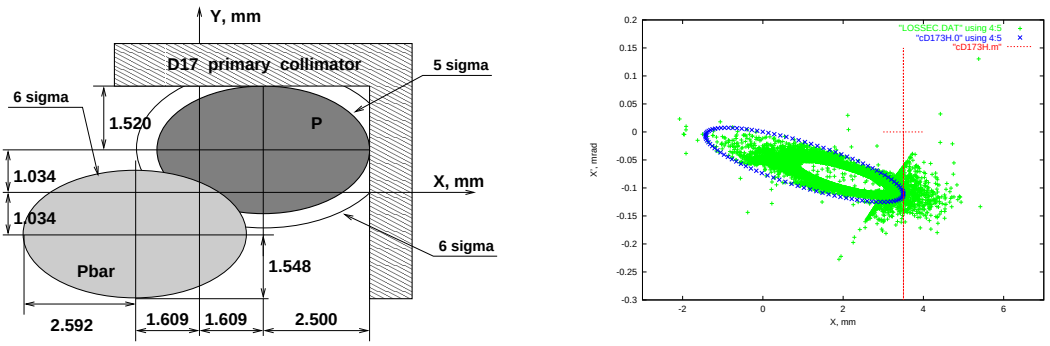

Figure 2: Proton beam primary collimator D17(1) (left) and horizontal phase space at secondary collimator D17(3) (right).

After the first interaction with a primary collimator, large amplitude particles are intercepted by the secondary collimators, but some fraction survives and will interact with the primary collimator again on the next turns. With primary collimators at 5σ and secondary ones at 6σ, it takes 2-3 turns on average to intercept an outscattered particle with the secondary collimator. Particles with amplitudes $<6\sigma$ are not intercepted by the secondary collimators and survive for another 20-30 turns until they increase amplitude in the next interactions with a primary collimator. The halo tail is extended beyond 6σ. Halo distribution in the Tevatron aperture is shown in Fig. 3.

Beam loss distributions in the Tevatron are presented in Fig. 4 for proton and antiproton directions. Antiproton collimators intercept 6×10^6 p/s in the proposed system, that is five times lower than the proton scraping rate and results in about five times lower accelerator-related background in DØ and BØ. Beam loss rates in the IRs are 35% lower if one puts the secondary collimators at 5.5σ, but one needs to verify if such a 0.5σ offset is reliable and stable.

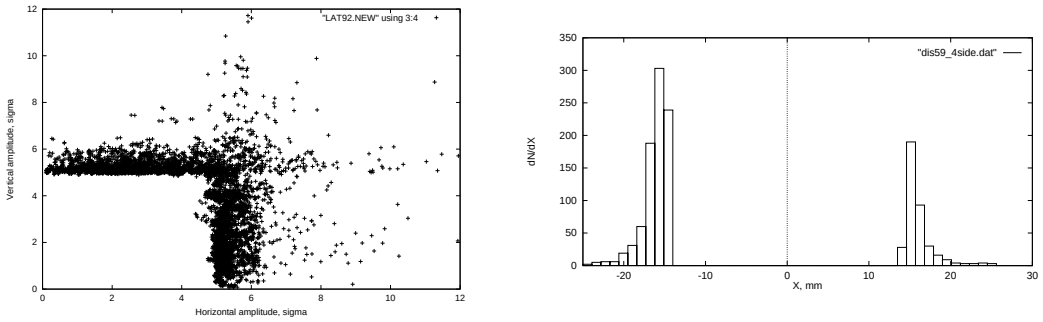

Figure 3: Proton beam halo in the Tevatron aperture (left) and its distribution at DØ quadrupole spectrometer Roman pots positioned at 8σ (right).

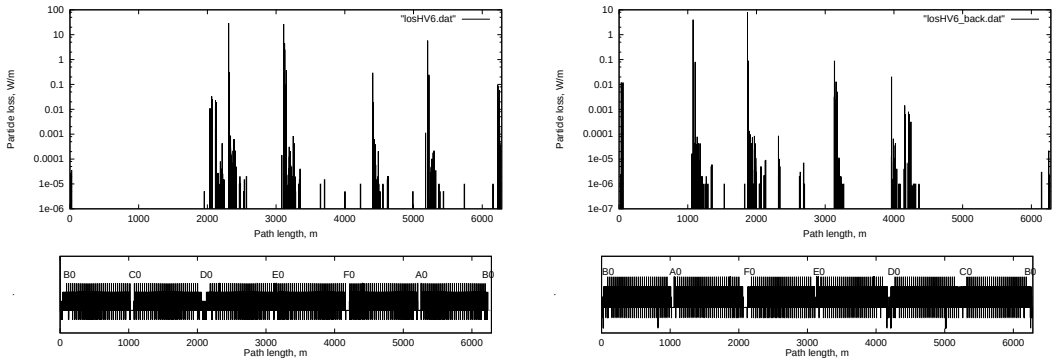

Figure 4: Beam loss distributions in the Tevatron for proton (left) and antiproton (right) directions.

3 Detector Interface Issues

At superconducting hadron colliders the mutual effect of the radiation environment produced by the accelerator and experiments is one of the key issues in the interaction region and detector development [9, 10]. The overall Tevatron and DØ and CDF detector performances are strongly dependent on details of such an interface. Efforts were made at Fermilab to optimize the DØ and BØ regions with proposed forward detectors in place for the Run II era.

3.1 DØ and CDF Forward Proton Detectors

Two new forward detectors have been recently proposed as new sub-detectors of the DØ and CDF collider detectors the for Tevatron Run II (see, e. g., [11]). These

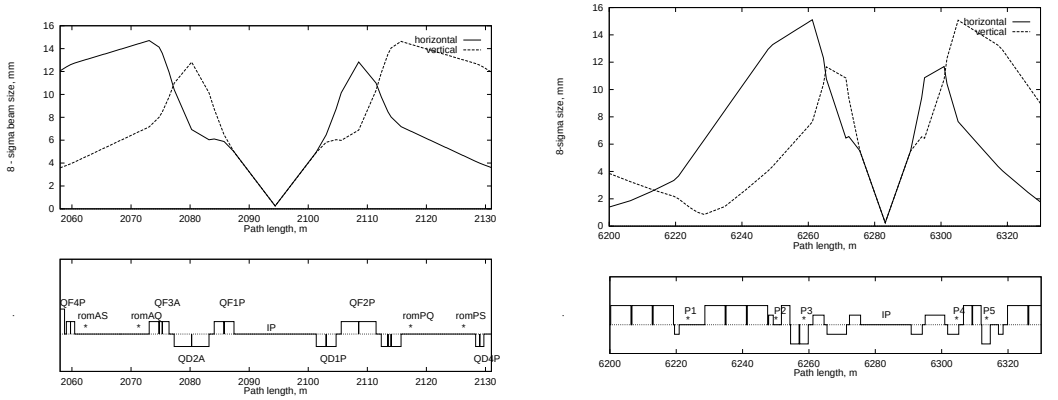

Figure 5: 8σ proton beam envelopes in DØ (left) and BØ (right). Roman pot locations are shown as romAS, romAQ, romPQ and romPS for DØ and P1–P5 for BØ.

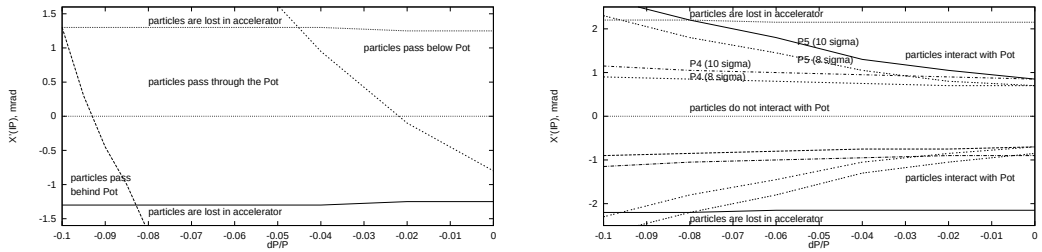

Figure 6: Horizontal acceptance of the CDF dipole spectrometer Roman pots (P1) at 10σ (left) and quadrupole spectrometer (P4, P5) at 8σ and 10σ (right).

detectors use the Tevatron magnets along with points measured on the track of the scattered proton to determine the proton momentum and angle. They consist of quadrupole spectrometers which tag outgoing protons or antiprotons with a minimum t and a dipole spectrometer which detects particles with a minimum Δp (see Fig. 5). The DØ FPD includes four Roman pot units (with four pots each) placed in the DØ straight section and two single units in the C48 location. The four units are upstream and downstream of the separators with 'A' referring to outgoing antiproton side and 'P' to outgoing proton side (Fig. 5). Each unit consists of four square 2×2 cm^2 detectors placed in horizontal and vertical planes on each side of the beam. The C48 units are placed only inside the accelerator orbit. The Roman pot positions are adjustable in the x or y directions and can be moved according to the beam halo conditions in the Tevatron.

Calculations of both DØ and CDF forward detector acceptances were done via tracking of particles ejected from the IP with various momenta and angles for several configurations. Horizontal acceptances of the CDF dipole and quadrupole spectrometers are shown in Fig. 6. The calculated values are quite acceptable and naturally go down with the Roman pots at larger distancies from the beam axis.

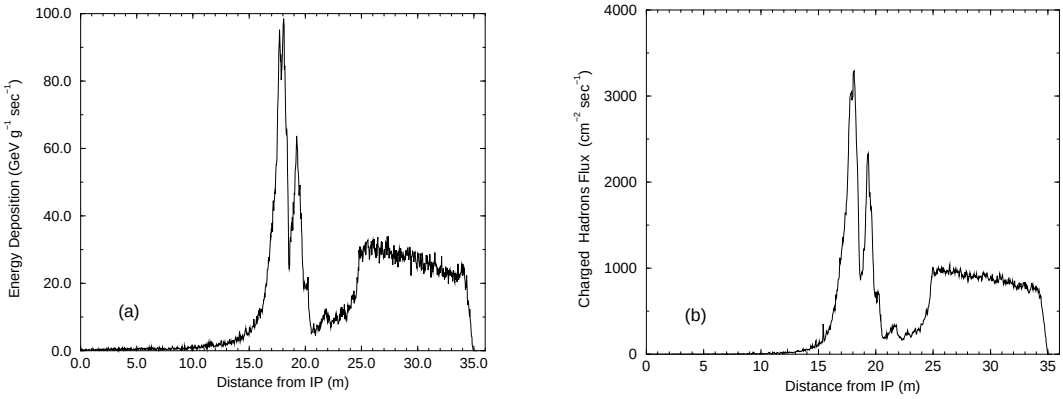

Figure 7: Beam loss source term in the BØ beam pipe: (a) energy deposition density; (b) high energy hadron flux.

3.2 Beam Loss and FPD Hit Rates

Realistic simulations of beam loss formation in DØ and BØ with beam collimation system and forward proton detectors in place followed by full simulations of induced hadronic and electromagnetic cascades were performed with the MARS-STRUCT code system [5, 6]. It turns out that the accelerator related background in the collider detectors is originated by beam halo loss in the Tevatron and FPD components within $\pm$50 m from the IPs (see Fig. 7 [12]). The limiting apertures are the β_{max}-region and the Roman pots placed at 8σ (DØ) and 10σ (BØ).

Some halo particles can pass through the Roman pot detectors several times inducing excessive hit rates in the pots themselfs and in the main BØ and DØ detectors. Calculations show that beam loss and hit rates are decreased by a factor of two by moving the Roman pots at DØ from $8\sigma_x$ to $9\sigma_x$. The price one pays is decreased FPD acceptance (see Fig. 6). Therefore, the Roman pot positions will be chosen to compromise the main detector background and the FPD acceptance.

Hit rates in the DØ and CDF FPDs depend strongly on the Roman pot distance to the beam axis. Table 1 gives halo hit rate in the FPDs for several combinations. The source term is driven by proton interactions with the primary collimators D17(1) and D49 and, at lower rate, with the secondary collimators D17(2,3), F17(2), EØ (1) and AØ. For the antiproton beam, the sources are the primary collimators F17(3) and F49 and, at lower rate, collimators F17(1,2), EØ (2), D17(2) and F48. The Roman pot detectors are at $8\sigma_x$ for the proton beam and $9.4\sigma_x$ for antiprotons. Moreover, the antiproton intensity intercepted by the collimation system is 5 times lower compared to the proton intensity. Therefore, antiproton background in the Roman pots amounts to only 2% of the total background, and backgrounds in the DØ detector due to Roman pots on the proton side are about two orders of magnitude higher compared to the antiproton side.

Table 1: Halo hit rate (in $10^5\ p/s$) at the DØ and CDF Roman pots for several secondary collimator positions. All CDF Roman pots and DØ dipole pots are at 10σ.

Secondary collim.	$5.5\sigma_{x,y}$	$6\sigma_{x,y}$	$7\sigma_{x,y}$	$6\sigma_{x,y}$
DØ pots	$8\sigma_{x,y}$			$9\sigma_{x,y}$
D1	0.44	0.94	2.46	1.01
D3	0.41	0.89	2.30	0.98
AS	2.86	5.67	17.9	3.23
AQ	2.69	5.27	16.5	2.91
P1(1)	2.38	3.92	7.91	4.40
P1(2)	2.48	3.77	7.49	4.26
P1(3)	2.13	3.58	7.52	3.97
P2	5.84	10.7	23.5	11.7
P3	4.18	8.38	17.2	8.68

3.3 Backgrounds in DØ and CDF

Calculated with MARS-STRUCT, accelerator-induced hit rates in both Fermilab collider detectors are in good agreement with measurements (see, e. g., [8, 12] and Fig. 8). With no Roman pots, the accelerator-induced background is at most a few % of the background from $p\overline{p}$ collisions [8]. The DØ sub-detectors most sensitive to accelerator-related background are the forward muon spectrometer and the SVTX vertex detector. MARS-STRUCT simulations were done for 10^{13} protons and 10^{12} $\overline{p}$ per bunch ($\mathcal{L}$=10^{32} cm^{-2}s^{-1}), combining the magnetic fields, pots, electrostatic separators, quadrupole and dipole magnets, tunnel, shielding and the near-beam DØ detector components. Typical results on neutron flux in the Tevatron tunnel and in the DØ forward muon system are shown in Fig. 9. One sees that with the 8σ FPD neutron fluxes are higher by about a factor of eight. A difference in charged particle fluxes, directly responsible for hit rates, is not so big. A ratio of hit rate in the forward muon chambers with FPD to that without FPD is calculated to be 4.5 for pots at 8σ and 1.5 for pots at 9σ, implying a total increase in background rates of at most 15% and 5%, respectively.

The situation is rather similar for the central detector. Figs. 10 and 11 show calculated with MARS-STRUCT-GEANT photon fluxes in the DØ SVTX with and without FPD for the Run II parameters [13]. One sees that the accelerator related flux being at maximum (r$\sim$5 cm) 0.3% of that due to $p\overline{p}$-collisions, is about ten times larger with FPD at 8σ. At larger radii (r$>$10 cm), all components of the accelerator background in the central detector are negligeble compared to ones from IP, because of the self-shielding by the detector body.

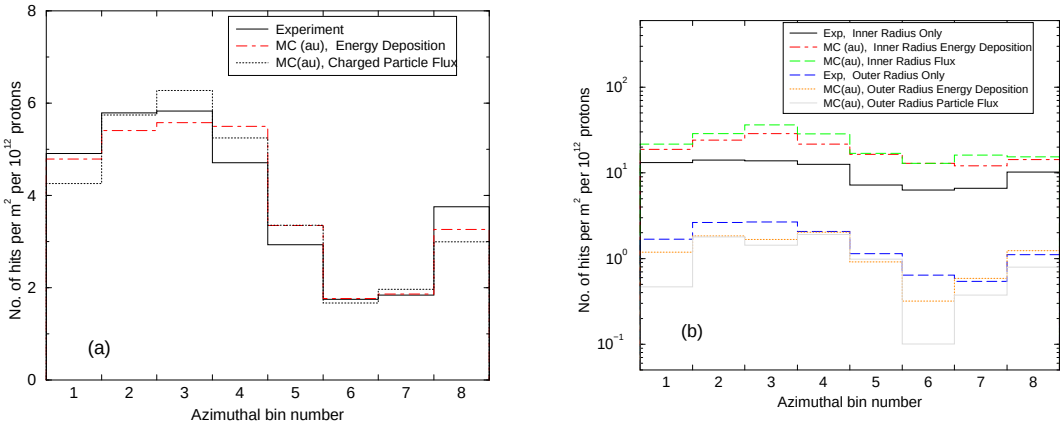

Figure 8: Calculated and measured azimuthal distributions of hits in the rear plane (Run I): (a) radially integrated; (b) inner and outer radial bins.

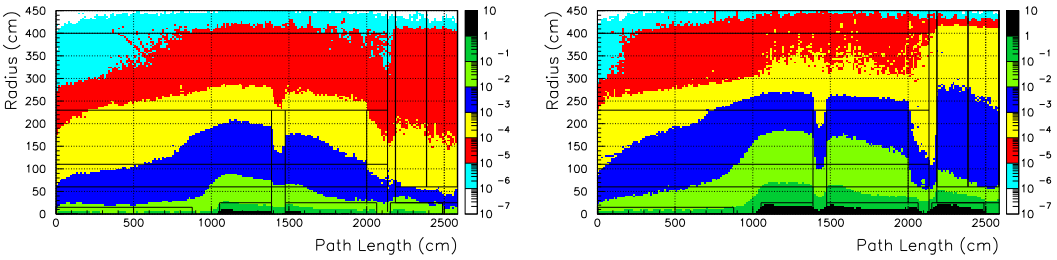

Figure 9: Neutron isoflux ($cm^{-2}s^{-1}$) in the DØ region with the collision hall at path length >2200 cm for baseline (left) and Roman pots at 8σ (right).

4 Conclusions

Beam losses in the Tevatron can be reliably controlled via a new sophisticated beam collimation system. Tracking studies show that both DØ and CDF FPDs have quite good acceptance for detecting scattered p and $\overline{p}$. Calculations confirm that halo background is not a problem for hard diffractive processes. Realistic MARS-STRUCT simulations show that the increase of background rates in the forward muon system due to beam halo interactions with Roman pots is at most 15% for pots at 8σ and a few % for pots at 9σ. With 1 ns time resolution in the pixel trigger counters and a 20 ns gate, one can easily distinguish between hits from halo and from $p\overline{p}$-interactions. MARS-GEANT simulations give very similar numbers for DØ SVTX.

5 Acknowledgments

We express our gratitude to Andrew Brandt, Mike Church and Sergei Striganov for useful discussions.

References

[1] D.A. Finley, J. Marriner and N.V. Mokhov, 'Tevatron Status and Future Plans', Fermilab–Conf–96/408, 1996.

[2] A. I. Drozhdin, M. Harrison and N. V. Mokhov, 'Study of Beam Losses During Fast Extraction of 800 GeV Protons from the Tevatron', Fermilab FN-418, 1985.

[3] M. Maslov, N. Mokhov and I. Yazynin, 'The SSC Beam Scraper System', SSCL-484, 1991.

[4] A. I. Drozhdin, N. V. Mokhov, R. Soundranayagam and J. Tompkins, 'Toward Design of the Collider Beam Collimation System', SSCL-Preprint-555, 1994.

[5] N. V. Mokhov, 'The MARS Code System User's Guide, Version 13(95)', Fermilab–FN–628 (1995).

[6] I. Baishev, A. Drozhdin and N. Mokhov, 'STRUCT Program User's Reference Manual', SSCL–MAN–0034 (1994).

[7] A. I. Drozhdin and N. V. Mokhov, 'Beam Loss Handling at Tevatron: Simulations and Implementations', IEEE 1997 Particle Accelerator Conference, Vancouver, BC, Canada, May 1997.

[8] J. Butler, D. Denisov, T. Diehl, A. Drozhdin, N. Mokhov and D. Wood, 'Reduction of Tevatron and Main Ring Induced Backgrounds in the DØ Detector', Fermilab–FN–629, 1995.

[9] N. V. Mokhov, 'Accelerator/Experiment Interface at Hadron Colliders: Energy Deposition in the IR Components and Machine Related Background to Detectors', Fermilab-Pub-94/085, 1994.

[10] A. I. Drozhdin, M. Huhtinen and N. V. Mokhov, 'Accelerator Related Background in the CMS Detector at LHC', Nucl. Instruments and Methods in Physics Research, **A381**, pp. 531-544, 1996.

[11] A. Brandt, A. Drozhdin, N. Mokhov et al., 'Proposal for Forward Proton Detector at DØ ', Fermilab, October 1996.

[12] O. E. Krivosheev and N. V. Mokhov, 'CDF Forward Shielding for Run II', Fermilab-TM-2045, 1998.

[13] A. Brandt, A. Drozhdin, N. Mokhov and S. Striganov, 'MARS-STRUCT-GEANT Studies of Backgrounds in Forward Proton Detector at DØ ', Fermilab, 1998 (in preparation).

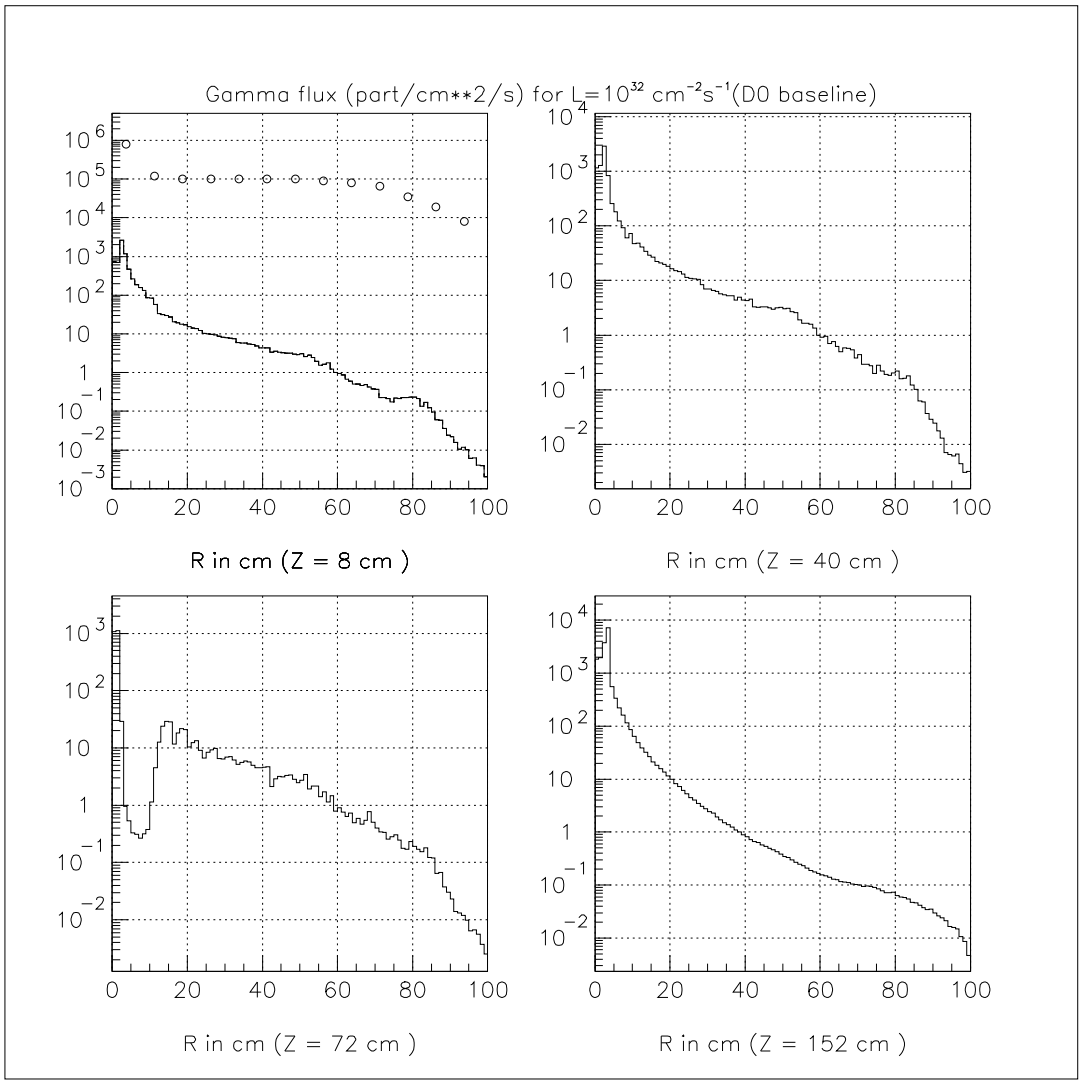

Figure 10: Radial distributions of accelerator-related photon flux in the DØ central detector at the four distances from IP without FPD detector. Symbols show the photon flux due to $p\overline{p}$ collisions.

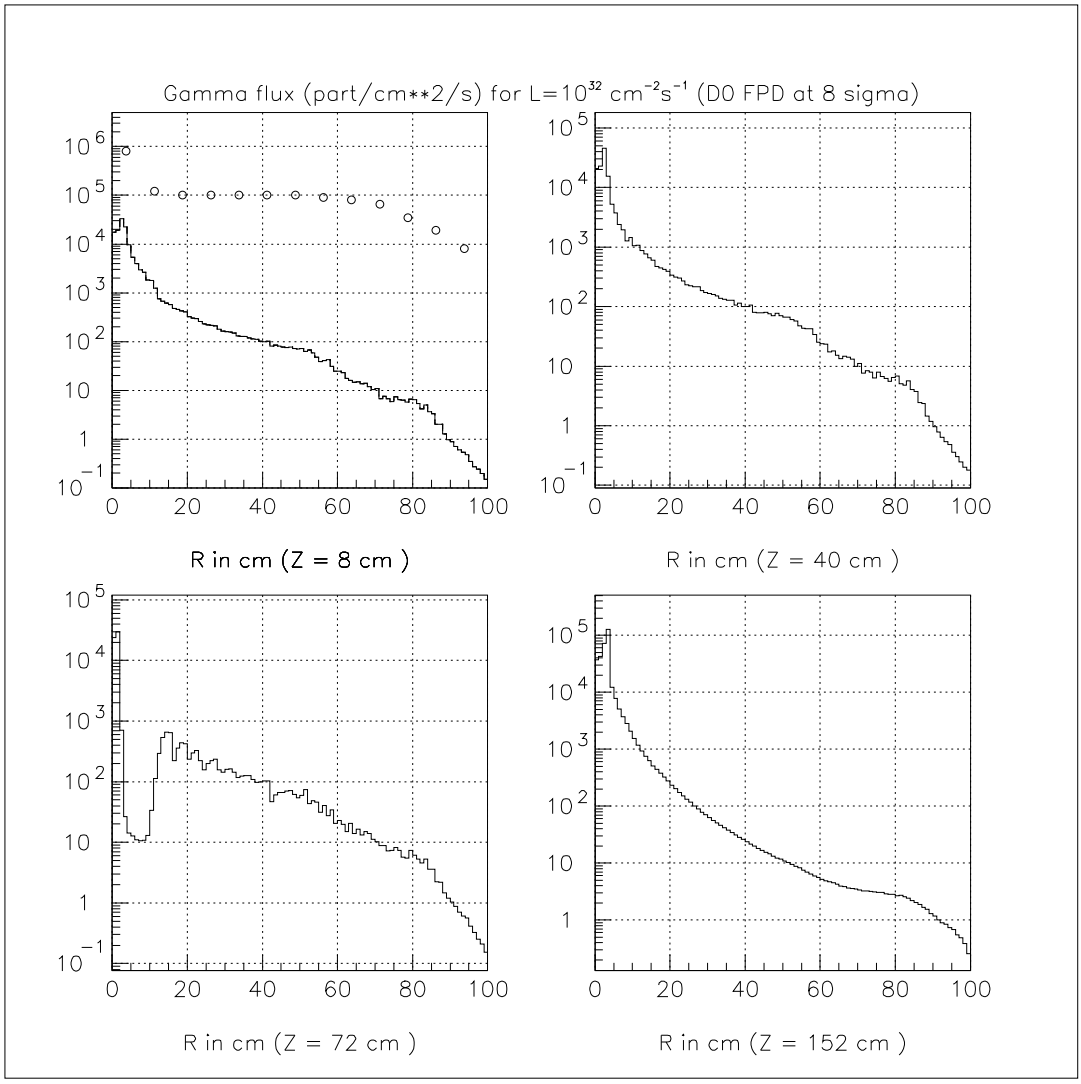

Figure 11: Radial distributions of photon flux in the DØ central detector at the four distances from IP with FPD detector at 8σ. Symbols show the photon flux due to $p\overline{p}$ collisions.